Online Dynamic Topology Type PV Grid - Connected Inverter for Efficiency Expansion

Mohanakumara S. D., Poshitha B.

M.Tech, Assistant Professor, Department of Electrical and Electronics Engineering, Adichunchanagiri Institute of Technology, Chikkamagaluru, Karnataka, India

Abstract: *Photo voltaic energy generation is a main purpose for clean and eco-friendly energy generation for growing demand in modern technological era. Apparently we have focus on making a grid source demand merging infrastructure as to make a dedicated H-Bridge and cascading-Bridge invertors for synchronous power generation and harmonic wave form distortions. In this paper, we focus on making an efficient PV grid system for dynamic load sharing and topological change management according to the demand. The paper also demonstrates the graphs and power consummation v/s power optimization rations with a MATLAB Simulink model.*

Keywords: CM-GCI, HB-GCI, PV-GGS, MC PWM, THD

1. Introduction

In today's environment, hydraulic power generation has failed to meet the demand ratio of growing population and thus researchers has moved they focus towards development of PV cells and technology. PV produces a lower cost power generation model and also it incorporates the green electricity principals.

In practical scenarios we have seen a distortion in production of constant output with PV simulation due to insignificant technological approaches. Many researchers have taken PV technology as a field for development and significant growth. Currently the demand is served under various grid topologies and hence in this paper we focus towards making an efficient grid infrastructure for making a better photo voltaic cell energy utilization. Photo voltaic grid power generation system (PV GGS) is widely used to optimize the power generation issues under inverter terminologies.
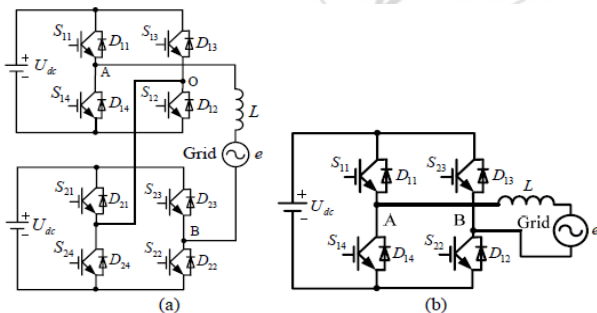

Figure 1: Schematics of CM-GCI and HB-GCI. (a) CM-GCI, (b) HB-GCI

2. Background Work

In this paper we shall mainly focus towards online topological behavior of the PV GGS system under H-Bridge and Cascaded Inverter environment. Apparently we also focus on power generation and dissipation with a graphical representation.

All the PV-GGS above are based on traditional power electronics technique and there exists the following problems:

1. The larger input range of PV-GGS, in order to obtain the safety and stability, the power level of the power components and filter inductor are selected from the maximum output power. While the filter inductor is designed from the requirement that the grid current total harmonics distortions (THD) should meet the special standards even under the minimum grid current amplitude conditions. A bigger filter inductor value is required. It results in lower system utilization, higher volume and cost.

2. Over a wide operation range, the inverter topology remains unchanged; all of the power switches involved in the system is always under working state, resulting in a large amount of loss, and the European efficiency decreasing obviously.
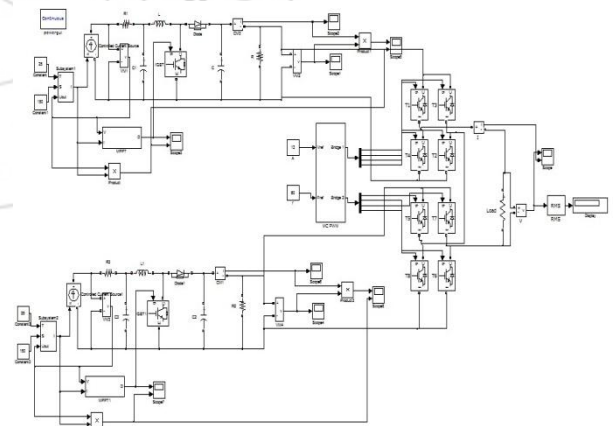

Figure 2: Simulink Model for Efficient Expansion of PV Grid Invertors with Dynamic Topological Infrastructure
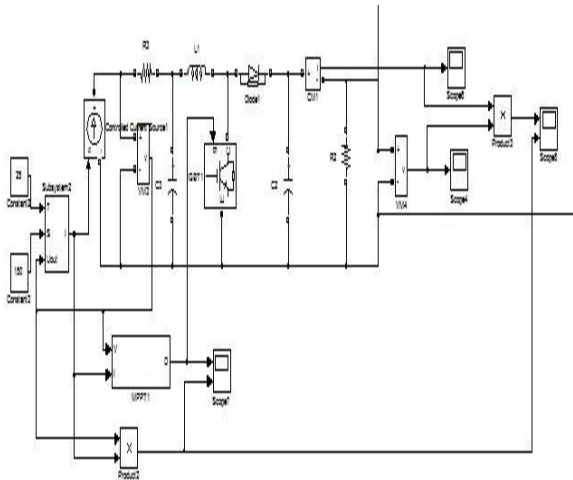
Figure 3: Grid Circuitry for PV GGS

3. Experimental Analysis

On the note for studying and developing an efficient system with dynamic topological changes according to the demand requirements is shown in Fig 1. The circuitry analysis consists of two way grid system as shown in Fig 2. The Grid for PV GGS consists of two way source charger for maximum and minimum power accommodation under normal and hybrid scenarios.

The major power generation is pulsed with a MPPT unit with minimal triggering voltage. A complimentary circuit is designed for voltage satisfaction with looped circuit. A detailed arrangement of invertors is shown in Figure 4 for dynamic topological alignment.
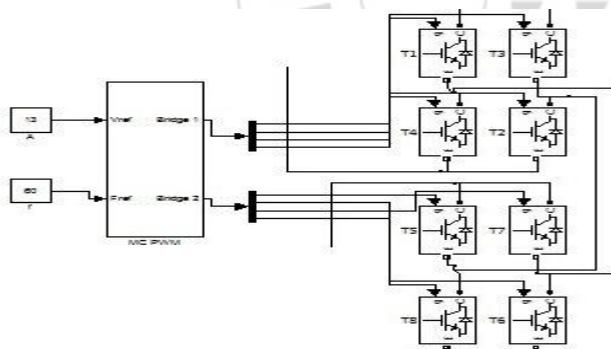

Figure 4: Dynamic Topological Inverter Arrangement

Under MATLAB Simulink modeling we have created a simulated environment for voltage based dynamic topological adjusting inverter circuit. The power efficiency is computed and recorded. The main contribution of this paper is proposing an online variable topology to obtain the goals above. The proposed OVT-GCI is based on the five-level CM-GCI. Two H-bridge inverters are connected in series with a bidirectional power switch S_{con} connecting the negative terminals of the two inverters. When S_{con} is off, the topology is a traditional five-level CM-GCI. When S_{con} is on, meanwhile, $S13$ and $S21$ are on and $S12$ and $S24$ are off; the positive and negative terminals of the two dc sources are connected, respectively. The reason of callingthe inverter as "equivalent HB-GCI mode" is that, compared with the standard HB-GCI, some additional power switches are

introduced. In the following, the working process of the equivalent HB-GCI is analyzed, and then, the additional conduction loss is calculated to evaluate the practicability and advantage of the proposed OVT-GCI.

The simulation is paused for time t=1 min and thus the following recording graphs are observed. The Fig 4 demonstrates charging of voltage sources at grid A and thus serves a major purpose for serving the demand at load.The voltage demand serving from grid A is shown in Fig 5, A higher stabilization is made after 0.5 for a slot of 1. With a regular offset of 0 and constant simulating voltage of range 160 to 175.
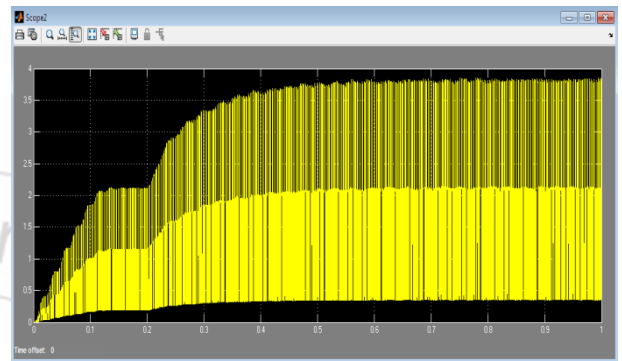

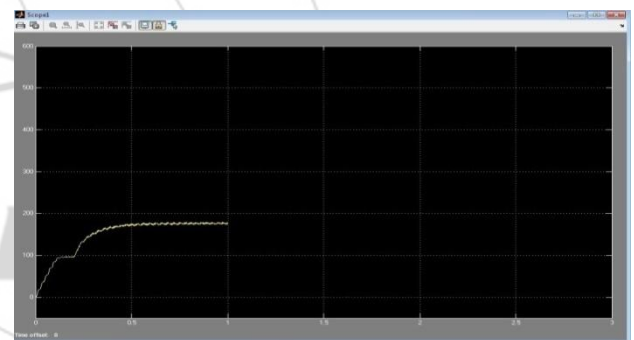**Figure 4:** Power Charging at Major Grid Unit

Figure 5: Voltage generation at Grid A1

The regular demand is served from Grid A and hence the invertors work as H Bridge inverter and under irregular meeting demand loses are encounter suppressing the voltages and thus a supportive decision is made of dynamically shifting topology under cascading environment.

At the output of inverter the simulation is paused for time t= 2 min and thus the following recording graphs are observed. The figure 6 represents the conduction pulses of eight IGBT and one bi-directional control switch which is called MC PWM control, which is represented for the switching action of the corresponding IGBT. The system is so arranged for closed loop using PI controller. Figure 7 represents the inverter output that is load voltage, load current and modulation signal, which is in the form of ac signal. The generated voltage by the photo-voltaic array is not constant which is variable by time. So that the variable generated DC voltage is arranged at the input side of the inverter, which is in the range of 150-230 V DC.

4. Pulse Width Modulation (MC PWM)

The inverter consists of total eight IGBT's, these IGBT's are switched ON and OFF at particular instant for changing mode of operation of the inverter. For loss less switching operation the efficient gate pulses are required. So that in this project it is implemented in MC PWM technology for efficient gate pulses, the switching operation is performing as for the following table I, II and III and the corresponding graph is shown in figure 6.

Table 1: Number of conduction-state power components of various output voltages of HB-GCI

Device	2Vdc	Vdc	0	-Vdc	-2Vdc
Number of IGBT	4	3	2	3	4
Number of diode	0	1	2	1	0

Table 2: Number of conduction-state power components of various output voltages of CM-GCI

Device	2Vdc	Vdc	0	-Vdc	-2Vdc
Number of IGBT	4	3	2	3	4
Number of diode	0	1	2	1	0

Table 3: Number of conduction-state power components of various output voltages of HB-GCI

	S	S1	S2	S3	S4	S5	S6	S7	S8
Vdc	ON	ON	-	-	-	-	ON	-	-
-Vdc	ON	-	-	-	ON	-	-	ON	-
Number of conduction-state power components of various output voltages of CM-GCI									
Vdc	-	ON	ON	-	-	-	ON	-	D8
2Vdc	-	ON	ON	-	-	ON	ON	-	-
-Vdc	-	-	D2	-	ON	-	-	ON	ON
-2Vdc	-	-	-	ON	ON	-	-	ON	ON

5. Inverter Output Voltage and Current

At the output of inverter the simulation is paused for time t= 2 min and thus the following recording graphs are observed. Figure 7 represents the inverter output that is load voltage, load current and modulation signal, which is in the form of ac signal. The generated voltage by the photo-voltaic array is not constant which is variable by time. So that the variable generated DC voltage is arranged at the input side of the inverter, which is in the range of 150-230 V DC. The output side of the inverter that consists of AC voltage and current waveform according to the two modes of inverter operation. The average voltage and current of cascaded inverter is slightly less than the average voltage and current of H-bridge inverter, this is shown in the graph.

Average voltage of cascaded inverter = 230 V
Average current of cascaded inverter = 2.25 A
Average voltage of H-bridge inverter = 240 V
Average current of cascaded inverter = 2.35 A

6. Total Harmonic Distortion (THD)

The figure 8 represents the graph that measures the total harmonic distortion (THD) of a periodic distorted signal. The signal can be a measured voltage or current. The THD is defined as the root mean square (RMS) value of the total harmonics of the signal, divided by the RMS value of its fundamental signal. Figure 8 represents the graph of total harmonic distortion which is produced by voltage and current harmonics. For example, for currents, the THD is defined as;

Total harmonic distortion (THD) = I_H / I_F

Where

I_n = RMS value of the harmonic n

I_F = RMS value of the fundamental current.

The calculated voltage and current THD by the graph is ranging from 2.938% - 1.837%.

The total harmonic distortion is achieved in this project is less than 3%

The THD has a null value for a pure sinusoidal voltage or current. The THD of H-bridge inverter is more than the cascaded inverter.

7. Voltage and Current Losses

The various losses are produced in the proposed system, among those here that concentrating on only voltage and current losses of the overall system. The losses, which are produced by the system due to various reasons. The voltage and current losses are inversely proportional to the efficiency of the system. The figure 9 represents the graph of voltage and current losses waveform that shows, The voltage loss and current loss are produced by the each h-bridge inverter is 0.58 watt. Therefore there are two H-bridge inverter, hence by adding up both the losses that gets the total voltage and current losses are 1.16 watts.

8. Output Power, Input Power and Efficiency

The total efficiency of the system is calculated by the ratio of output power to the input power by using the simulated graph. Obviously the output power of the system is less than the input power, this is mainly due to the deference in types of power (DC at source and AC at demand side). The value of the power produced by the system and efficiency of the system is shown in the figure 10.

The output power of the system = 380.6 watt.
The input power of the system = 392.3 watt.
The efficiency of the system = (output power / Input power)*100 = 97.01%)
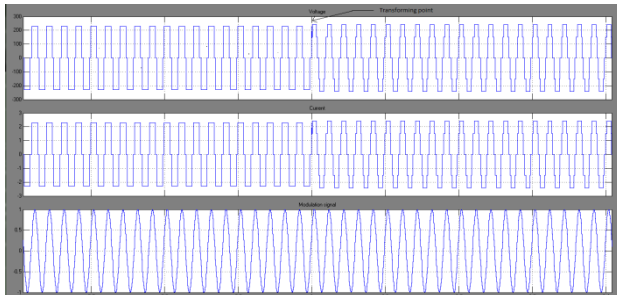
Figure 6: Switching Pulses
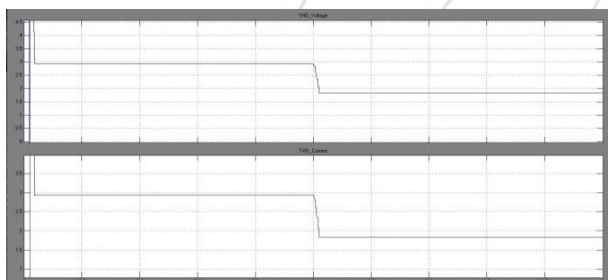

Figure 7: Voltage, Current and modulation signal

Figure 8: Voltage and Current THD

Figure 9: Voltage loss, Current Loss and Total Loss

Figure 10: Efficiency, Output and Input power

9. Conclusion

The electrical power system comprises of generation, transmission and distribution. Considering the generation system it is important to correct utilization of generated electrical power. This project represents the efficient utilization of generated electrical power of the photo-voltaic array generating system by reducing the losses and total harmonic distortions by using suitable electronic circuitry and improves the efficiency of the system as well.

Under our simulative study a detailed analysis is studied for various voltage demands merging with a dynamic topological approach for efficient power utilization. The paper also witnesses a wide improvement for demand satisfaction. The analysis results of CM-GCI and HB-GCI indicate that, the operation range of CM-GCI is wider while the efficiency is lower. Hence a simulative conclusion is made on working efficiently under topological switching. Throughout this project, the THD is 5% and it is limited within 3%. Efficiency of inverter is further improved. The European efficiency of CM-GCI is 95.8% and the European efficiency of the proposed topology is 97.01 % with an increase of 1.21 %.

References

[1] Fengjiang Wu, Bo Sun, Jiandong Duan and Ke Zhao "On-Line Variable Topology-Type Photovoltaic Grid-Connected Inverter", DOI 10.1109/TIE.2015.2405052.

[2] T. LaBella, W. Yu, J. Lai, M. Senesky, and D. Anderson, "A bidirectional-switch-based wide-input range high-efficiency isolated resonant converter for photovoltaic applications," *IEEE Trans. Power Electron.*, vol. 29, no. 7, pp. 3473–3484, Jul. 2014.

[3] T. V. Thang, N. M. Thao, J. Jang, and J. Park, "Analysis and design of grid-connected photovoltaic systems with multiple-integrated converters and a pseudo-DC-link inverter," *IEEE Trans. Ind. Electron.*, vol. 61, no. 9, pp. 4734–4745, Sep. 2014.

[4] J. Wu and C. Chou, "A solar power generation system with a seven level inverter," *IEEE Trans. Power Electron.*, vol. 29, no. 7, pp. 3454–3462, Jul. 2014.

[5] L. Zhang, K. Sun, H. Hu, and Y. Xing, "A system-level control strategy of photovoltaic grid-tied generation systems for European efficiency enhancement, " *IEEE Trans. Power Electron.*, vol. 29, no. 7, pp. 3445–3453, Jul. 2014.

[6] F. Ancuta, C. Cepisca, "Fault analysis possibilities for PV panels," in *Pro. International Youth Conference on Energetics*, Leiria, Portugal, Jul. 2011, pp. 1 - 5

[7] J. Storey, P. R. Wilson, and D. Bagnall, "The optimized-string dynamic photovoltaic array," *IEEE Trans. Power Electron.*, vol. 29, no. 4, pp.1768–1776, Apr. 2014.

[8] Y. Yang, K. Zhou, and M. Cheng, "Phase compensation resonant controller for PWM converters," *IEEE Trans. Ind. Informat.*, vol. 9, no.2, pp. 957–964, Sep. 2013.

[9] M. K. Ghartemani, "Linear and pseudolinear enhanced phased- locked loop (EPLL) structures,"

Paper ID: NOV163706

1388

IEEE Trans. Ind. Electron., vol. 61, no. 3, pp.1464–1474, Mar. 2014.

[10] Y. Huang, M. Shen, and F. Z. Peng, "Z-source inverter for residential photovoltaic systems," IEEE Trans. Power Electron., vol. 21, no. 6, pp. 1776–1782, Nov. 2006.

[11] IEEE recommended practices and requirements for harmonic control in electrical power systems, IEEE Standard 519-1992, 1992

Paper ID: NOV163706

1389